Large, High-Quality DIAMOND From Brazilian Kimberlite

Diamonds were first discovered in alluvial secondary deposits of Brazil by gold miners circa 1725. Brazil became the world's premier diamond source for more than a century, until diamonds were located in South Africa. Meanwhile, the search for primary sources continued. More than 1,100 kimberlite pipes have been discovered in Brazil, most of them concentrated near alluvial deposits. So far, only five have been tested using current exploration technology. The Braúna kimberlites in Bahia State were found in the early 1990s, but it was not until 2005 that modern sampling techniques revealed their potential. In 2014, the Lipari Mining Company developed an open-pit mine on one of the Braúna kimberlite pipes, the first primary deposit diamond mine in South America.

Recently, the New York laboratory analyzed a 50.8 ct (10.10 g) near-colorless crystal of high quality submitted by Lipari. The rough was analyzed both before and after faceting as part of GIA's new "Mine to Market" service, which documents a diamond's journey from rough crystal to final faceted gemstone. The rough had a dodecahedral habit, resulting from resorption into mantle fluids post-growth. GIA determined it to be type Ia (bearing nitrogen aggregates). It was relatively clean, with no large mineral inclusions or fractures, indicating that it could be faceted into a high-clarity gem diamond. From this rough crystal, a 20.1 ct round brilliant cut diamond with I color and VS_2 clarity (figure 1) was produced and resubmitted as the second stage of the Mine to Market service. DiamondView images documented the growth structure of this crystal, allowing comparison of the rough to the final faceted gemstone.

Figure 1. Left: A Brazilian kimberlite yielded a 50.8 ct rough type Ia diamond with a dodecahedral habit, the result of resorption. Right: This 20.1 ct round brilliant with I color was cut from the Brazilian rough.

Mid-FTIR spectra taken from both the rough and the faceted stone (figure 2, left) confirmed it to be type Ia, with a moderate concentration of hydrogen; the two spectra overlay each other very closely. Also collected were UV-visible absorption spectra. Typical cape spectra were observed, including the peaks at 415 and 478 nm that are common for a diamond of this color (figure 2, right). Under cross-polarized light, strong "tatami" strain patterns (figure 3) indicated strong plastic deformation during and after growth. These geological processes can limit the ability of such large crystals to survive transport to the earth's surface, adding to the rarity of this impressive diamond.

Although the round brilliant was of high clarity, a small colorless euhedral crystal was observed under the table facet. The morphology of this crystal identified it as a garnet, and Raman analysis using 514 nm laser excitation confirmed it as pyrope garnet (Mg-, Al-rich) (figure 4).

DiamondView images of both the rough crystal and the final faceted gem

Editors' note: All items were written by staff members of GIA laboratories.

Gems & Gemology, Vol. 53, No. 3, pp. 360–368.

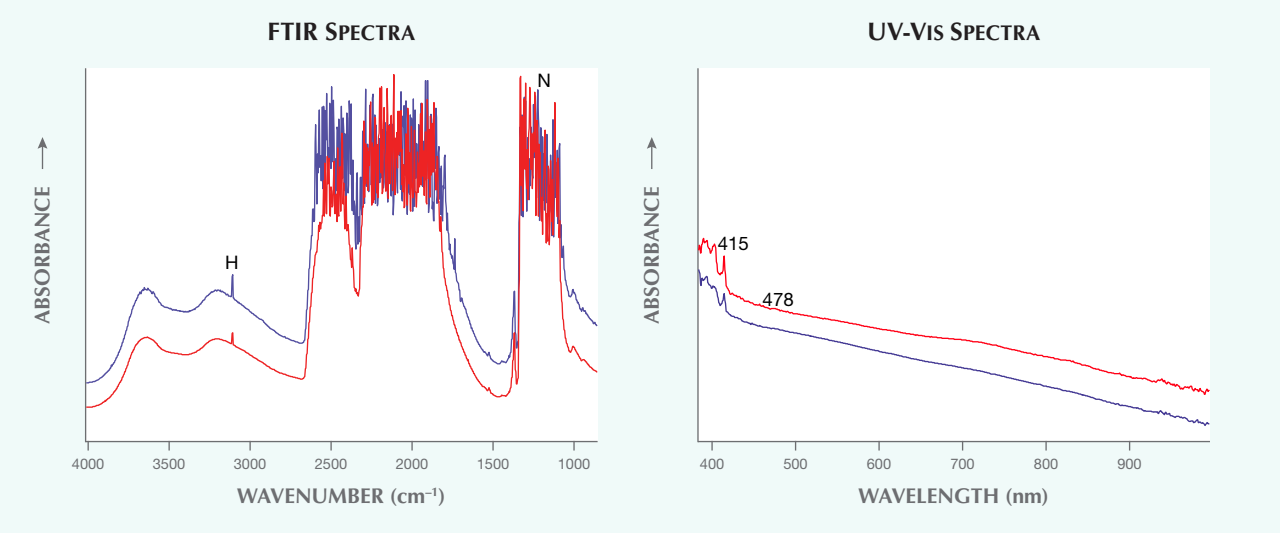

Figure 2. Mid-infrared and UV-visible spectra of the rough diamond crystal (blue trace) and finished round brilliant (red trace) showed that it was a type Ia cape diamond. The spectra are offset for clarity.

revealed similar growth patterns, along with the strong blue fluorescence typical for type Ia diamond (figure 5). These observations further confirmed that the stone was cut from the notable 50.8 ct rough crystal.

Lipari is currently exploring 20 other primary kimberlite sources in Brazil, and similarly impressive diamonds may be forthcoming.

Paul Johnson, Heather Smith, and John King

EMERALD with Mobile Inclusion

Multiphase inclusions are key indicators when identifying emeralds and determining their origin. Gemologists look for the jagged three-phase inclusions in stones of Colombian origin or blocky two-phase inclusions in Brazilian or Zambian emerald. These multiphase inclusions typically require higher magnification and considerable maneuvering of the emerald to get a precise view.

Recently, the Carlsbad laboratory received a 9.02 g rough emerald from Lucas Fassari (Costa Mesa, California). The rough had an eye-visible mobile inclusion (figure 6) consisting of a CO_2 gas bubble and salt crystals suspended in a fluid. The emerald was identified using a handheld spectroscope and op-

Figure 3. Tatami strain patterns, typical for a type Ia diamond, indicate that the crystal experienced plastic deformation during and possibly after growth.

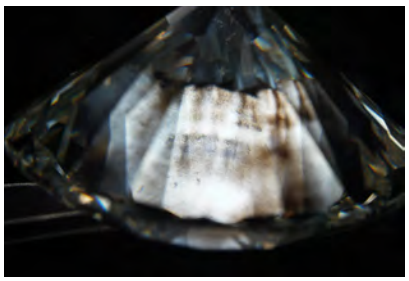

Figure 4. The Raman spectrum obtained from the diamond's crystal inclusion identifies it as a pyrope garnet (Mg-, Al-rich). Inset: The well-formed crystal is approximately 20 microns in diameter.

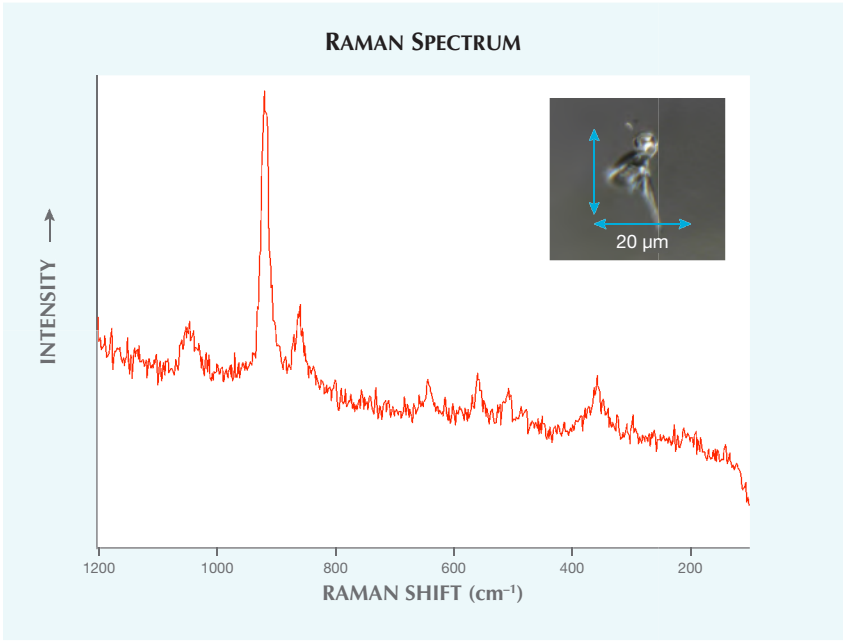

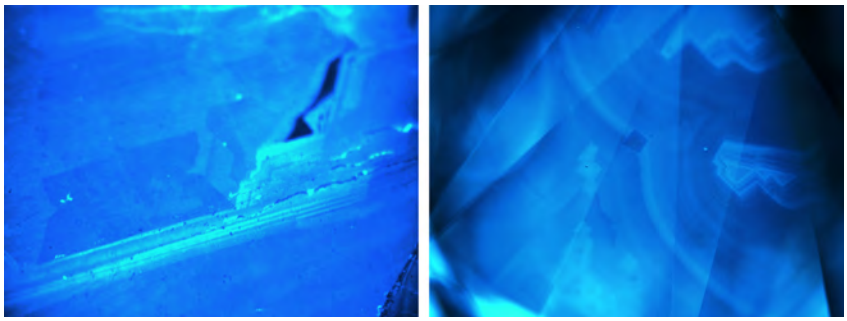

Figure 5. Identical growth structures and fluorescence patterns in DiamondView imaging confirm that the original 50.8 ct rough diamond crystal (left) yielded the finished 20.1 ct diamond (right).

tical properties. It was determined to be of Colombian origin by its jagged three-phase inclusions and crystals that had characteristics of pyrite and calcite. The mobile inclusion was quite large in relation to the rough emerald, which measured 28.76 × 14.82 × 12.83 mm, including its calcite and shale matrix. The CO_2 bubble measured approximately 4 × 3 mm.

Mobile inclusions of this size are captivating to observe, and to see one in an emerald adds more allure to the piece (see video at http://www.gia.edu/gems-gemology/fall-2017-labnotes-emerald-mobile-inclusion). Cutting this specimen into a faceted gemstone would lose what makes this rough emerald unique.

Nicole Ahline

Figure 6. This 9.02 g rough emerald contains a prominent eye-visible mobile inclusion.

Ethiopian Precious OPAL with a Dyed Brown Bodycolor

Brown opal exhibiting play-of-color has been previously reported (M.L. Johnson et al., "Opal from Shewa Province, Ethiopia," Summer 1996 *G&G*, pp. 112–120) and can occasionally be found in the marketplace as "chocolate opal."

Recently, a 17.15 ct semi-transparent oval cabochon with brown bodycolor and strong play-of-color (figure 7, left) was submitted to the Carlsbad laboratory for identification services. Basic gemological observation and properties confirmed that the stone was opal. The spot refractive index was 1.41. The opal displayed hydrophane behavior by absorbing water, which was easily observed during microscopic examination (Fall 2013 Lab Notes, pp. 175–176).

While this specimen's properties were consistent with Ethiopian opal with a natural brown bodycolor, it was necessary to confirm that the color was not the result of dye, since this was hydrophane-type material (N. Renfro and S.F. McClure, "Dyed purple hydrophane opal," Winter 2011 *G&G*, pp. 260–270). Meticulous examination showed that the brown color conformed to the surface, indicating that it was in fact the result of dyeing after the stone had been fashioned. The uneven bodycolor was difficult to detect because of the stone's transparency and strong play-of-color. Careful microscopic examination with strong transmitted and diffused white lighting revealed very subtle color concentrations in pits and uneven blotchy brown patches on the surface (figure 8), which confirmed that the brown color was artificially induced. Interestingly, the back of the stone was almost white in the center and brown along the edge

Figure 7. A 17.15 ct brown dyed precious opal from Ethiopia (left). The back of the stone was almost white, which suggests that it had been re-polished after dyeing (right).

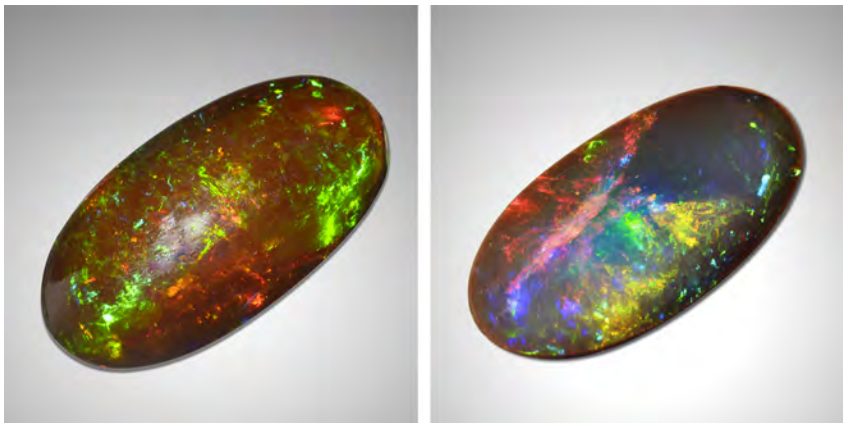

(see figure 7, right), showing clear surface-conformal brown color. This suggests that the back of the stone was repolished after dyeing, which would have removed the dark brown rind in the process.

On the brown side, the opal showed an unusual chalky greenish yellow color when examined under long-wave UV light, possibly due to the dye. Advanced gemological analysis with Raman spectroscopy revealed a natural opal spectrum that was free of any peaks pertaining to foreign substances. Energy-dispersive X-ray fluorescence (EDXRF) did not detect manganese, which is the cause of brown color in Ethiopian opal.

Although dyed opal is often easy to identify, this brown dye looked natural, and the color of the stone did not change after hydrophane testing. While the dye was difficult to detect on the top surface of this stone, its back fortunately appeared to have been repolished, offering additional evidence of dye. When examining opal, it is important to consider carefully whether it could be dyed, especially if it is hydrophane material with a color that occurs naturally.

Jonathan Muyal

Figure 8. Uneven color is observed with the help of strong transmitted and diffused lighting; the blotchy darker brownish area is the result of dyeing. Field of view 3.57 mm.

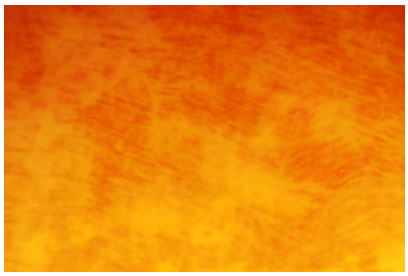

Figure 9. Both of these precious opals show an unusual and attractive bodycolor. The opal on the left is a 6.71 ct transparent pink cushion brilliant. On the right is a 2.37 ct transparent orange round brilliant.

Unusual Bodycolors of Precious Opal

Two faceted loose stones with unusual bodycolors (figure 9) were recently submitted to the Carlsbad laboratory for an identification report. The first, a 2.37 ct transparent round brilliant, showed a weak to moderate play-of-color with irregular color patches and brushstrokes. It exhibited an attractive orange bodycolor (similar to the hue of some *padparadscha* sapphires) and a light degree of haziness. Careful microscopic examination revealed turbid orangy clouds and waves of coarse particles. The larger specimen, a 6.71 ct transparent cushion brilliant, also displayed a weak to moderate play-of-color but more of a pink bodycolor. A similarly hazy appearance from clouds of orangy red particles and tiny black inclusions was also observed (figure 10).

Standard gemological properties were consistent with opal. The orange and pink stones both had a specific gravity of 2.03, with refractive indices of 1.442 and 1.445, respectively. Both were inert to long-wave and short-wave UV light. No indication of clarity enhancement, color treatment, or dye was observed in either. The two stones were therefore identified as natural opal with natural color.

A single drop of water placed on the surface of each stone was observed under direct transmitted light with the microscope in brightfield mode. The opals showed no indication of porosity and did not absorb the water, suggesting they were not hydrophane material (Fall 2013 Lab Notes, pp. 175–176). Crazing was not seen in either opal.

Advanced gemological testing with EDXRF showed properties consistent with natural opal ($SiO_2 \cdot nH_2O$), but also the presence of Fe, most likely from the clouds of particles.

While the exact cause of these pink and orange bodycolors is unknown, the minute inclusions might be influencing the perceived color.

Our gemological observations confirmed the natural origin. However, further study on additional samples would be required to better understand the cause of color in these unique opals. They were reported to be from Mexico, but the author could find no reference consistent with this material.

Jonathan Muyal

Figure 10. The pink opal contained clouds of tiny orangy red particles. Field of view 2.88 mm.

Natural Freshwater "Fish" PEARL

The increased availability of freshwater cultured pearls in the market has brought their natural counterparts to the attention of collectors and the trade. Most natural freshwater pearls have been obtained from European waters and in the United States from rivers in the Mississippi Valley. A natural pearl occurs without human intervention and takes on the characteristic color and surface properties of the mollusk in which it forms. Freshwater pearls, whether cultured or natural, are attractive due to a wide variety of distinctive shapes, hues, and overtones. The New York lab recently examined a unique fish-shaped brownish orange pearl measuring 21.34 × 6.28 × 2.81 mm and weighing 2.12 ct (figure 11).

Figure 11. A 2.12 ct natural freshwater pearl with the form of a fish.

The entire nacreous surface was composed of overlapping platelets. We observed no indications of work, such as polishing, that is sometimes performed to improve a pearl's appearance. One end was wider and more rounded, which bore an uncanny likeness to a fish's head, with an "eye" and "mouth" also discernible. The lustrous orient along the body narrowed to a rounded point, resembling iridescent fish scales on a tail. Natural pearls are often baroque, and American freshwater pearls in particular are often found as elongated "wing" pearls (J.L. Sweaney and J.R. Latendresse, "Freshwater pearls of North America," Fall 1984 *G&G*, pp. 125–140). EDXRF chemical analysis and observation of X-ray fluorescence showed higher levels of manganese, proving that the pearl formed in a freshwater mussel. No indications of treatment such as dyeing or coating were detected under magnification or using advanced analytical procedures. Real-time microradiography and X-ray computed microtomography (μ-CT) analysis revealed clear natural growth structures that conformed to the pearl's shape. 3D rendering of the μ-CT data (figure 12) showed a remarkable likeness to a small fish swimming.

Although this is not the first pearl GIA has examined that bears a resemblance to a living creature (see Fall 2015 Lab Notes, pp. 319–320), it is nonetheless an extraordinary and rare formation that mirrors the form of a fish in surprising detail.

Sally Chan and Emiko Yazawa

Elements in Synthetic Overgrowth On Flux-Heated RUBY and Beryllium-Diffused Sapphire

Heat treatment of rubies and sapphires at high temperatures sometimes leaves redeposition caused by the partial dissolution of the corundum in the crucible; this is referred to as synthetic overgrowth (Fall 2002 GNI, pp. 255–256). GIA's Tokyo laboratory recently had the opportunity to test a red oval mixed cut weighing 2.00 ct and an orange round mixed cut weighing 0.89 ct, both of which showed signs of synthetic overgrowth after testing.

Standard gemological testing and advanced testing including chemical

Figure 12. 3D software rendering of X-ray μ-CT data revealed the pearl's uncanny likeness to a fish.

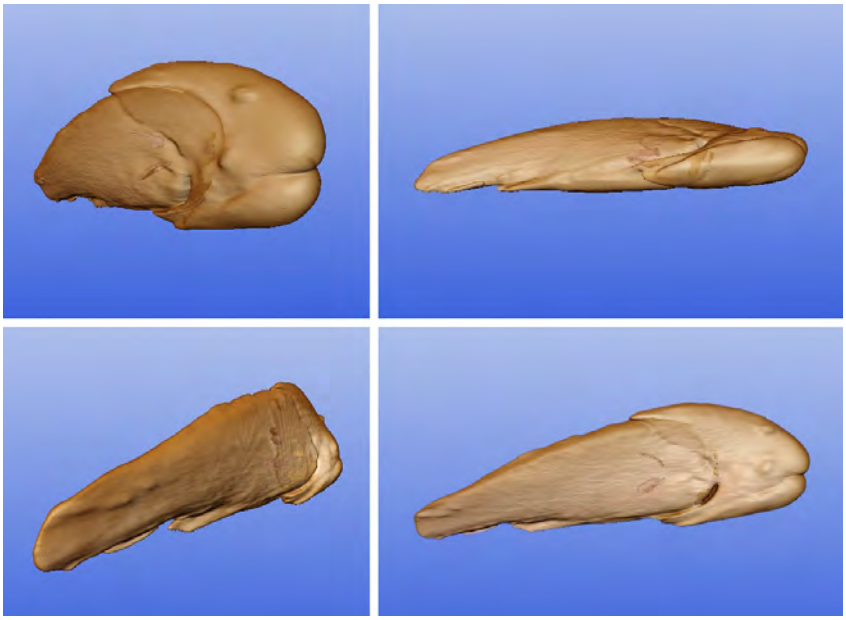

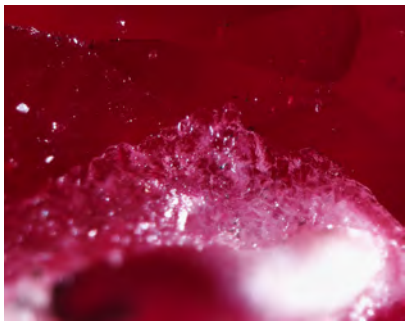

Figure 13. Synthetic overgrowth on the surface of a heated Burmese ruby. Field of view 1.50 mm.

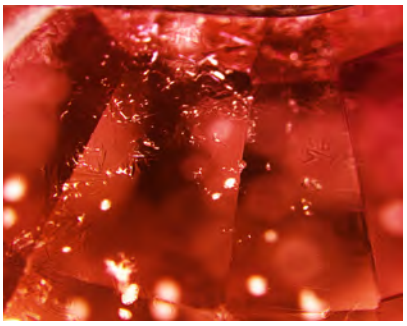

Figure 14. Synthetic overgrowth on an orange beryllium-diffused sapphire. Field of view 1.60 mm.

analyses revealed that the red oval was a heated ruby of Burmese origin with moderate flux residues in fissures. The orange round was identified as a beryllium-diffused sapphire. Both stones had synthetic overgrowth around the girdles and/or cavities (figures 13 and 14) that could be confirmed by different reactions under cross-polarized light. We tested the overgrowths with laser ablation–inductively coupled plasma–mass spectrometry (LA-ICP-MS) with calibration using NIST 612 and 610 standards.

The chemical compositions of these synthetic overgrowths were different from those of corundum; they also varied between the samples. Sodium (9980 ppmw), calcium (40,100 ppmw), magnesium (84,400 ppmw), and silicon (23,400 ppmw) were extremely high in the overgrowth on the flux-heated ruby; beryllium (36,650 ppmw) was extremely high and silicon (909 ppmw) very high in the overgrowth on the beryllium-diffused sapphire (table 1). Boron was detected only in the overgrowth on ruby (59 ppmw). Aluminum was not quantified since it was used as an internal standard. However, the high aluminum signal indicated that the overgrowth contained corundum and/or alumina-related material.

Flux is used for artificial heat treatment of rubies, and there are many types of fluxes such as oxides, borates, silicates, molybdates, and fluorides, as well as various combinations of materials (J.L. Emmett, "Fluxes and the heat treatment of ruby and sapphire," Fall 1999 *G&G*, pp. 90–92). During flux-assisted heat treatment with or without diffusion, material from the surface of the corundum as well as the alumina crucible and inclusions will dissolve to some degree into the molten flux. On cooling, the flux becomes supersaturated in alumina and crystallizes out onto the nearest convenient surface, often on the stones themselves (J.L. Emmett et al., "Beryllium diffusion of ruby and sapphire," Summer 2003 *G&G*, pp. 84–135). Uncommon elements for corundum such as sodium, calcium, and silicon obtained from the overgrowth on heated ruby in high concentration indicate that the overgrowth was mainly derived from fluxes. These elements are comparatively insignificant for the overgrowth on beryllium-diffused sapphire. On the contrary, extraordinarily high beryllium in the overgrowth on Be-diffused sapphire indicates deposition of this additional element in the treatment. Other elements, such as magnesium and zirconium (detected at moderate to high levels), and metals such as nickel, copper, zinc, and lead (detected from both overgrowths at lower levels) may be from the inclusions or the flux.

LA-ICP-MS results (table 1) also indicate that the ruby could be misidentified as Be-diffused since the overgrowth contains a certain amount of beryllium, a possible by-product of the furnace. It is important for gemologists to check other elements such as magnesium, silicon, and calcium in order to confirm that LA-ICP-MS was performed on the overgrowth.

Yusuke Katsurada

TABLE 1. Elements in heated ruby and Be-diffused sapphire and their synthetic overgrowths detected by LA-ICP-MS (avg. concentration in ppmw[a]).

	Heated ruby		Be-diffused sapphire	
Element	Stone	Overgrowth	Stone	Overgrowth
Be	bdl[b]	5.00	8.86	36,650[c]
B	bdl	59.0	bdl	bdl
Na	bdl	9980	bdl	10.6
Mg	10.5	84,400	61.1	328
Si	bdl	23,400	bdl	909
K	bdl	1790	bdl	bdl
Ca	bdl	40,100	bdl	bdl
Ni	bdl	104	0.42	6.20
Cu	1.71	50.1	bdl	8.34
Zn	bdl	64.0	bdl	12.7
Zr	0.04	27.6	bdl	296
Pb	bdl	93.7	bdl	0.15

[a] *All detection limits are below 4 ppmw except for Si (heated ruby: 113.5 for stone, 104.1 for overgrowth; Be-diffused sapphire: 93.3 for stone, 80.0 for overgrowth) and Ca (heated ruby: 16.95 for stone, 15.79 for overgrowth; Be-diffused sapphire: 16.95 for stone, 15.79 for overgrowth).*
[b] *bdl: below detection limit*
[c] *These values were linearly extrapolated with pulse-analog linear dynamic range measurement of the instrument.*

Figure 15. This 1.76 ct synthetic diamond was submitted with a fake GIA inscription (partially redacted for privacy) of an actual GIA report number for a natural diamond.

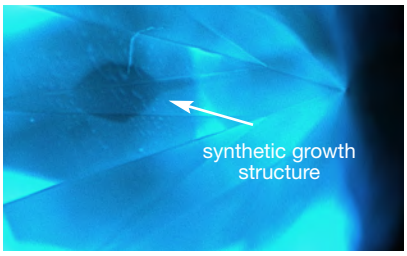

Figure 16. DiamondView imaging showed the synthetic growth structure and blue phosphorescence typical of HPHT-grown synthetic diamonds.

SYNTHETIC DIAMOND

Fraudulently Inscribed to Match Natural Diamond Report

Improvements in diamond growth technology and methods have led to a noticeable increase in colorless synthetic gem diamonds in recent years. Concerns in the diamond industry focus on laboratory-grown diamonds not being properly disclosed or even being sold as natural stones. Through careful examination and analysis, gemological laboratories can separate natural from synthetic diamonds. Occasionally, however, fraud is involved in attempting to conceal a gem's identity. The Carlsbad laboratory witnessed such an attempt.

On this occasion, a round brilliant cut (figure 15, left) was submitted for an updated diamond grading report. Its girdle was inscribed with an actual GIA report number issued in 2015 (figure 15, right). The older report was for a natural, untreated diamond and contained the following grading information: 1.74 ct, round brilliant cut, D color, Excellent cut grade, and VVS_1 clarity. Upon grading, the new submission was described as a 1.76 ct round brilliant cut with F color, Excellent cut grade, and VS_1 clarity. Moreover, our screening processes determined that the newly submitted sample needed additional testing to determine its origin. This examination revealed it to be an HPHT-grown synthetic diamond. Synthetic cuboctahedral growth structure and phosphorescence were clearly visible in DiamondView imaging (figure 16).

Aside from the observed discrepancies in weight (1.74 vs. 1.76 ct), color (D vs. F), and clarity (VVS_1 vs. VS_1), FTIR spectra clearly showed that these were not the same diamond. The natural diamond from the original report was type Ia with aggregated nitrogen impurities, while the new one was type IIb with boron impurities (figure 17). Careful examination of the report number inscribed on the synthetic diamond revealed a font different from the one used by GIA, proving that it was not an authentic inscription.

While most synthetic diamonds that come to the laboratory are properly disclosed, some are submitted out of concern that a stone presented as natural might be synthetic. Rarely do we encounter the type of blatant fraud described here. It is important for the industry and public to exercise caution, because these types of misleading practices do occur. We believe the submitting client noticed inconsistencies with the GIA report information and sent it to the lab for an updated report. If any doubt exists or some aspect of a diamond (such as an inscription) seems odd, the stone should be sent to a gemological laboratory for verification.

Christopher M. Breeding and Troy Ardon

Screening of Mounted Melee Using The GIA iD100

As previously reported in the *G&G* Lab Notes section (Fall 2016, p. 307), significant amounts of melee-size

Figure 17. FTIR absorption spectra revealed that the synthetic diamond was type IIb, whereas the fraudulently inscribed report number referred to a natural type Ia diamond. The spectra are offset for clarity.

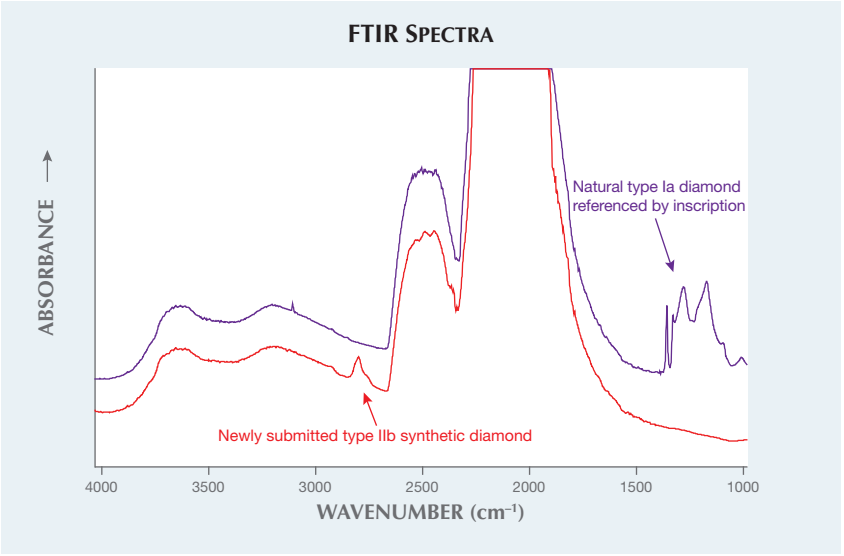

synthetic diamonds, both HPHT- and CVD-grown, are being manufactured for the jewelry industry. Over the past year, we have seen more instances of synthetics incorporated into finished jewelry pieces (e.g., Fall 2017 Lab Notes, p. 239).

Recently in GIA's New York laboratory, we examined a diamond ring with 100 colorless melee side stones, each about 0.5 mm in diameter (figure 18). Using the new GIA iD100 screening device, we were able to screen these melee. The device uses sophisticated spectroscopy technology to distinguish natural diamonds—either loose or mounted—from synthetics and simulants. The operator simply points the probe at a diamond, and the result is given within two seconds. Out of the 100 melee from this ring, one stone was referred by the GIA iD100 for further testing (figure 19).

Upon further examination, the stone was determined to be a type IIa diamond (no detectable nitrogen impurity). Examination in the De Beers DiamondView instrument revealed strong phosphorescence to short-wave UV radiation, typical for HPHT-grown synthetic diamonds (figure 20). Further examination using photoluminescence (PL) spectroscopy detected a very weak silicon impurity and a very high concentration of nickel, often a catalyst used to grow HPHT synthetic diamonds.

This ring offered an excellent example of how the GIA iD100 can quickly screen very small mounted diamonds and accurately detect any synthetics or even simulants.

Figure 18. A diamond ring with 100 melee side stones incorporated into the setting.

Figure 19. One stone, about 0.5 mm in diameter, was referred by the GIA iD100 for further testing. The inset photo shows a prototype of the iD100.

Paul Johnson and Stephanie Persaud

Flux-Grown Pink SYNTHETIC SAPPHIRE with Unusual Crystal Inclusions

The Carlsbad laboratory recently received a saturated pink cushion mixed cut, mounted in a ring, that measured 14.02 × 10.35 × 6.24 mm (figure 21). Standard gemological testing yielded a refractive index of 1.760–1.768 and a weak ruby spectrum using a handheld spectroscope, properties consistent with pink sapphire. The stone displayed a strong orange fluorescence under long-wave UV and an odd chalky orangy yellow fluorescence under short-wave UV. While orange fluorescence is not unusual in pink sapphires, the intensity and the chalky yellow reaction were suspicious.

Microscopic examination revealed a single hexagonal, dark reflective platelet (figure 22); numerous transparent, colorless tabular to rounded doubly refractive crystals (figure 23) that showed interference colors under crossed polarizers; and a small fingerprint composed of elongated tubules. Observation in immer-

Figure 20. The referred melee displayed strong phosphorescence to short-wave UV radiation, as is typical of HPHT-grown synthetic diamonds.

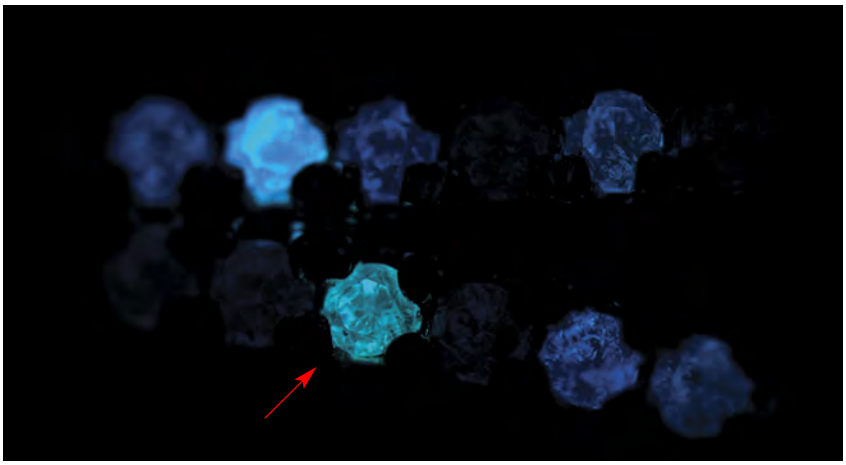

Figure 21. This pink stone proved to be a flux-grown synthetic sapphire with unusual crystal inclusions.

sion showed some weak, straight orange and pink zoning. This inclusion scene could easily be mistaken for natural as the transparent crystals bore a certain resemblance to zircon, a common inclusion in natural sapphires and particularly pink sapphires from Madagascar. The dark reflective platelet, which was presumably platinum, and odd fluorescence prompted further investigation.

The synthetic nature of the sapphire was confirmed using LA-ICP-MS. High amounts of Pt were detected, which would support a flux synthetic growth process. Small amounts of Fe and Be were present; Ga, Ti, and V were not detected. This chemical profile also supports synthetic sapphire.

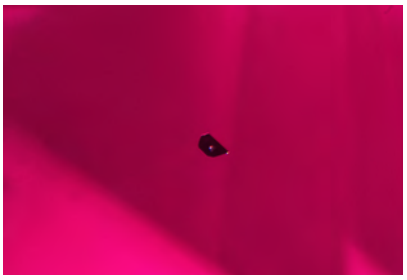

Figure 22. This dark reflective platinum platelet observed in the pink synthetic sapphire is a common inclusion in flux-grown synthetic corundum. Field of view 1.82 mm.

Transparent crystals of possible chrysoberyl ($BeAl_2O_4$) have been previously cited in flux-grown synthetic corundum (R.E. Kane, "The gemological properties of Chatham flux-grown synthetic orange sapphire and synthetic blue sapphire," Fall 1982 *G&G*, pp. 140–153). In that case, Chatham stated that heavy concentrations of beryllium were added to the original aluminum oxide formula, which would explain the presence of those crystals. In our pink sapphire, none of the crystals reached the surface, so we were unable to identify them with Raman spectroscopy. Small amounts of beryllium were detected, so chrysoberyl could be a possibility in this case as well.

Figure 23. The abundance of transparent crystals and crystal clusters could easily be mistaken for a natural inclusion scene in a pink sapphire from Madagascar. Field of view 1.79 mm.

The presence of these natural-looking crystals combined with the general lack of other inclusions for a stone of this size, particularly diagnostic flux fingerprints, could make correct identification very difficult for gemologists without access to advanced instrumentation. This is one case where advanced testing in a well-equipped gemological laboratory was necessary to make a conclusive identification.

Claire Ito

PHOTO CREDITS
Jian Xin (Jae) Liao—1; Paul Johnson—3, 5, and 20; Robison McMurtry—6, 7, 9, and 21; Jonathan Muyal—8; Nathan Renfro—10, 22, and 23; Sood Oil (Judy) Chia—11, 18, and 19; Emiko Yazawa—12; Yusuke Katsurada—13 and 14; Troy Ardon—15.

For More on Lab Notes

To watch video of the mobile inclusion in emerald (pp. 361 362), go to https://www.gia.edu/gems gemology/fall 2017 labnotes emerald mobile inclusion, or scan the QR code to the right.